Solar Energy Materials & Solar Cells 235 (2022) 111452

Contents lists available at ScienceDirect

Solar Energy Materials and Solar Cells

journal homepage: www.elsevier.com/locate/solmat

Effect of gas atmospheres on the interactions between liquid silicon and coated graphite substrates

Rania Hendawi *, Lars Arnberg, Marisa Di Sabatino

Department of Materials Science and Engineering, NTNU, 7491, Trondheim, Norway

ARTICLE INFO

Keywords:
Wettability
Coating
Stability
SiC
Si_3N_4

ABSTRACT

Interactions between the gas atmosphere, liquid silicon, Si_3N_4 coating, and graphite are of great interest for photovoltaic silicon applications. However, previous studies focus more on the wetting of silicon on coated substrates rather than the coating stability and interaction with furnace atmosphere. Here we report on the coating deoxidation and the liquid silicon behavior at different compositions of nitrogen, carbon monoxide, and argon. In-situ melting experiments were performed with solar grade silicon samples in various gas compositions. The results showed a rapid reaction between molten silicon and carbon monoxide that led to the formation of a silicon carbide layer at the liquid free surface. This layer retains the silicon droplet at the early stage of wetting and prevents silicon infiltration and spreading. Furthermore, CO gas prohibits the self-reduction of SiO_2 in the coating and the reduction by graphite. On the other hand, nitrogen accelerates the wetting of silicon as it favors the formation of highly wetted silicon nitride compound at the triple line of the droplet. A slight increase in the decomposition rate of silica content in the coating was observed with the introduction of nitrogen to the furnace. The influence of the morphology and the growth of nitride and carbide layers on the wettability was elucidated in detail. The results were supported by Raman spectroscopy and thermodynamic calculations.

1. Introduction

Graphite as a refractory material has unique properties that promote its use in many metal casting applications. In silicon crystallization processes, graphite crucibles must be coated to prevent reactions with the melt. However, in this case, the interactions between solid, liquid, and gas phases in the system must be carefully considered. Graphite is coated with a 300–500 μm layer of silicon nitride, which is considered the least detrimental material among all other silicon compounds that acts as a barrier between liquid silicon and graphite crucible. Typically, silica is added to the coating to suppress the adhesion between the molten silicon and the coating [1,2]. During melting, SiO_2 decomposes because of its interaction with other components in the system, such as dissolution in the melt, reacting with the silicon nitride, or reduction by the graphite [1,3,4]. Usually, the heating process takes place under a vacuum up to 800 °C and then argon is introduced to minimize the melt contamination of carbon, nitrogen, and oxygen [5]. Yuan et al. [6] have proposed using nitrogen gas as a cheap substitute for argon during the melting and solidification of silicon. They have also claimed that nitrogen can be utilized as a doping source for the silicon ingots where the concentration of dopants is controlled by adjusting the flow rate and the partial pressure of nitrogen in the furnace [6].

Some studies have reported on the Si_3N_4 coating stability and the mechanisms of SiO_2 reduction under vacuum and argon atmosphere at the melting temperature of silicon [7,8]. They have suggested that the coating deoxidizes due to the reaction between Si_3N_4 and SiO_2 (self--reduction reaction), which results in nitrogen and SiO gases evolution. CO gas is also expected in the furnace atmosphere owing to the direct contact between graphite substrate and SiO_2 content of the coating as well as the reaction between graphite and SiO gas. Many reactions in the Si–O–N–C system can affect the efficiency of the crystallization process in terms of coating stability, crucible durability, and ingot quality. The reactions that take place at the liquid-coating interface such as dissolution of coating components into the melt have been extensively investigated by Refs. [1,9] on a quartz substrate, and by Ref. [10] on graphite substrates. These reactions can significantly affect the wetting and infiltration of liquid silicon as reported by Ref. [9]. The reactions at the coating-graphite interface that result in the silica reduction and evolution of CO gas have been recently reported in Refs. [3,10]. Furthermore, the interactions between the liquid silicon and the gas

* Corresponding author.
E-mail address: rania.hendawi@ntnu.no (R. Hendawi).

https://doi.org/10.1016/j.solmat.2021.111452
Received 9 September 2021; Received in revised form 15 October 2021; Accepted 18 October 2021
Available online 17 November 2021

phase can alter the liquid behavior during melting. The dissolution of nitrogen and carbon monoxide in liquid silicon contaminates the melt, and forms precipitates above the saturation limit [9,14]. Several studies have attempted to measure the solubility of nitrogen, carbon, and oxygen in liquid silicon as a function of temperature [11–14]. Moreover, some studies have reported on the surface tension of liquid silicon in different atmospheres via contactless oscillating drop techniques or on uncoated substrates as summarized in Ref. [7], which contribute to a better understanding of the silicon liquid behavior in different atmospheres.

The existence of carbon monoxide and nitrogen gases in the furnace atmosphere is expected to alter the behavior of liquid silicon in contact with coated graphite. However, the effect of these gases on the coating stability, and hence the kinetics of the silicon wetting have not been reported in the literature. Furthermore, the decomposition of SiO_2 should be also studied in different atmospheres. The interactions between liquid silicon and the gas phase can also alter the wetting behavior of silicon. While several studies have attempted to explain the mechanism and kinetics of the gas-solid reaction such as silicon nitridation below the melting point of silicon [15,16], no studies are reported on the kinetics of liquid silicon-gas reactions.

Our study aims to investigate in depth the influence of the gas atmosphere on the coating decomposition and the liquid behavior. This work includes three major areas: (i) the wetting kinetics of silicon on coated graphite substrates in different gas compositions, (ii) the influence of CO, N_2 on the coating deoxidation rates, and (iii) the kinetics and the mechanism of silicon carbide and silicon nitride formation as a result of the gas-liquid reactions. Gases are mixed according to the desired ratios and systemically added to the inlet during melting of solar grade silicon on coated graphite substrates in a furnace where the shape of the droplet is recorded.

2. Materials and methods

The in-situ melting experiments were performed in a graphite sessile drop furnace which was equipped with a digital video camera (Sony XCD-SX910CR) to record the change of the droplet shape over time. 100 mg solar-grade silicon samples (8N-purity) were placed on the coated graphite substrates and heated under vacuum (10^{-6} mbar) to 800 °C for degassing. Then argon (6 N purity) was introduced with a flow rate of 2.5 l/min during heating to 1450 °C. Upon melting, the desired gases were mixed by different ratios as listed in Table 1 and introduced to the furnace. The flow rates of the inlet gases were carefully calculated to reach the desired concentration within one minute after the drop melting. The gas flow rate upon melting was 0.7 l/min. Due to the reactions between nitrogen, carbon monoxide, and silicon samples below the melting temperature, heating was perfomed in argon atmosphere. For instance, the reaction between solid silicon and nitrogen is highly favorable at temperatures over 1000 °C, which in turn can prevent the melting of the samples as expressed in the following reaction:

$$3Si_s + 2N_2 \leftrightarrow Si_3N_4 \quad (1)$$

The oxygen level in the furnace was measured by a zirconia sensor that was attached to the gas outlet. The oxygen partial pressure in the furnace upon melting was 10^{-19} atm, which is crucial to avoid the formation of an oxide layer on the molten silicon drop as the critical oxygen partial pressure for oxide-free droplet is $10^{-18.5}$ atm. The in-situ melting experiments are categorized based on the gas composition into three main groups as listed in Table 1

Isostatic graphite samples were preheated at 120 °C and then sprayed by a mixture of silicon nitride powder, colloidal silica, polyvinyl alcohol, and distilled water. The initial oxygen concentration of the coating was 8 wt.%. The coating thickness was 200 ± 30 μm.

The morphology and structure of the samples were studied using SEM Zeiss Ultra 55. Energy Dispersive X-ray Spectroscopy (EDS) was used to identify silicon carbide and silicon nitride particles that formed in the silicon droplets. Electron Probe Microanalysis (EPMA) JXA-8500F was used to measure the deoxidation depths of the coatings by scanning the oxygen concentration across the coating thickness. To investigate the interfaces of the coated samples after melting, Raman scanning was performed using a WITec alpha300 R with a 532 nm laser. Raman spectra were obtained after 8 accumulations for 10 s from 50 to 3500 cm^{-1}.

Table 1
Experimental matrix.

	Gas composition (%)		
	P_{N2}	P_{CO}	P_{Ar}
Group A	10	0	90
	50	0	50
	100	0	0
Group B	0	1	99
	0	2	98
	0	3	97
	0	4	96
	0	5	95
Group C	99	1	0
	98	2	0
	97	3	0
	96	4	0
	95	5	0

3. Results and discussion

3.1. Wetting behavior

Fig. 1 shows the effect of the nitrogen concentration in the gas atmosphere on the apparent contact angle between the silicon droplet and the coated graphite substrates. All the tested graphite samples were coated with a mixture of silicon nitride and colloidal silica to achieve 8 wt.% oxygen in the coating. Fig. 1 also shows that increasing the nitrogen concentration in the furnace seems to accelerate the decline in the contact angle until it reaches the equilibrium values. For instance, the sample that was melted under a 50% nitrogen concentration in argon reached the equilibrium contact angle after approximately 780 s of melting, while the sample that was melted in a 100% nitrogen stabilized after 480 s of melting. The equilibrium contact angle ranges between 40° and 50°, which agrees with the equilibrium contact angle between silicon and silicon nitride that has been reported in Refs. [2,17]. This

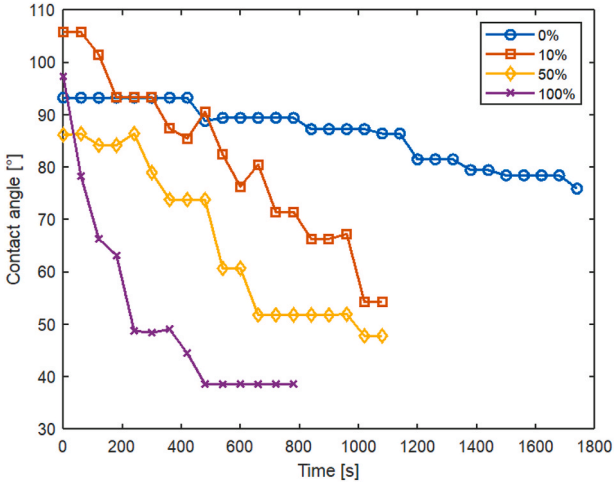

Fig. 1. Wetting behavior at different nitrogen concentrations in argon at 1723 K. The graphite substrates are coated with a 200 ± 30 μm of Si_3N_4. The initial oxygen concentration in the coating is 8 wt.%. The legend represents the nitrogen concentration in the gas atmosphere.

change in the wetting behavior can be attributed to a possible decrease in the surface energy of the liquid silicon in the nitrogen atmosphere. However, Millot et al. [18] have reported a slight increase in the surface tension of silicon samples that were melted in a nitrogen atmosphere in contrast to the ones obtained in argon. Therefore, it is more likely that the dramatic influence of nitrogen on the wettability results from the reactions between nitrogen and the coating components as well as the reactions with liquid silicon as will be discussed in detail in the next sections.

The wetting experiments that were performed under different carbon monoxide concentrations in argon atmosphere reached the equilibrium contact angle within the first 60 seconds. No apparent change in the contact angle was reported. To clearly understand the effect of CO gas, Fig. 2 shows the effect of 3% CO on the droplet geometry at 1723 K on an unoxidized sample compared to the one that was obtained in argon. Upon melting in argon, the contact angle of the silicon droplet decreases rapidly since the coating contains no anti-wetting products such as SiO_2 and Si_2N_2O. The addition of CO gas to the furnace maintains the droplet at the early stage of wetting where no further change in its geometry is observed.

Another set of experiments were applied to study the effect of nitrogen and carbon monoxide gases on wettability as illustrated in Fig. 3. The high reactivity of CO with liquid silicon is reported even at the lowest tested CO concentration in nitrogen atmosphere. The formation of SiC and Si_3N_4 particles on the top of the droplet prevents any interaction between silicon and coating and holds the initial contact angle as clearly seen in Fig. 3.

3.2. Coating stability

The stability of SiO_2 in the coating plays a crucial role in the liquid silicon wetting behavior during the isothermal holding. The decomposition of SiO_2 results in silicon infiltration and wetting of the coated substrates [1,19]. In this section, we discuss the effect of the gas atmosphere on the oxygen depletion from the coating. The depth of the deoxidized coating was measured by EPMA oxygen line-scanning and the results are summarized in Fig. 4. The addition of CO gas to the furnace atmosphere reduces the deoxidation depth of the coating as shown in Fig. 4. The key point for explaining the influence of CO gas on the coating stability is first to understand the deoxidation reactions of the coating in an inert atmosphere. Fig. 5 shows the major deoxidation regimes in the coating that are resulted in the reduction of SiO_2. The three major reactions are explained below with the influence of CO gas on each reaction:

(i) Dissolution of SiO_2 into silicon melt as follows:

$$SiO_2 + Si_l \leftrightarrow 2SiO \quad (2)$$

This process is driven by the low oxygen concentration in the liquid silicon. Generally, SiO_2 dissolves into the melt and oxygen diffuses throughout the liquid and evaporates as SiO. When CO is introduced to the furnace atmosphere, CO dissolves in liquid silicon into carbon and oxygen atoms, which will lead to the liquid saturation of these two light elements. Approaching the saturation level of oxygen in the melt will eliminate the driving force of SiO_2 dissolution into the melt.

(ii) Deoxidation of the bulk coating by self-reduction reaction:

$$3SiO_2 + Si_3N_4 \leftrightarrow 6SiO + 2N_2 \quad (3)$$

The self-reduction of SiO_2 occurs in the bulk of the coating where there is no direct contact with the liquid silicon. The main driving force, in this case, is the low partial pressure of SiO in the furnace atmosphere. However, increasing the concentration of CO gas in the furnace will hinder this reaction as CO and SiO are thermodynamically related by the following reaction:

$$SiO + 2C \leftrightarrow CO + SiC \quad (4)$$

(iii) Reduction by graphite at the substrate-coating interface:

$$SiO_2 + 3C \leftrightarrow SiC + 2CO \quad (5)$$

Another important reduction reaction of silica occurs at the coating-substrate interface as shown in Fig. 5. The presence of CO gas in the atmosphere prohibits the forward reduction reaction of SiO_2 by the graphite at the coating-graphite interface as clearly seen in Fig. 6 a-b where there is no observed deoxidation of the coating at the coating-graphite interface.

Therefore, based on the foregoing discussions, introducing CO gas to the furnace atmosphere can successfully hinder the three reduction reactions of SiO_2. It should be noted that the deoxidation depths of the coatings at 1–5% CO in argon are measured at two intervals:10 and 30 minutes. The deoxidized depths of the coating are found equal at the two intervals (see Figure S1 in Supplementary Materials). This indicates that the deoxidation of silica under the droplet, in presence of CO in the atmosphere, is a transient step and no further deoxidation is expected. When the liquid silicon reaches the saturation level of oxygen, the deoxidation rate of the coating will be negligible.

Fig. 4 shows the measured deoxidized depths of the coating at different nitrogen concentrations. Increasing the nitrogen concentration in the furnace accelerates the oxygen depletion from the coating. The predominance diagram of the Si–N–C–O system at 1723 K indicates that increasing the partial pressure of nitrogen above $10^{-1.5}$ atm will stabilize the silicon nitride compound over the silicon oxynitride (see Supplementary materials Figure S2). In this case, the decomposition of SiO_2 will undergo an intermediate reaction and form Si_2N_2O which will in turn form silicon nitride as a final product. At the coating-substrate interface, no significant influence of the nitrogen gas on the reduction of SiO_2 by graphite is observed. The reactions between SiO_2 and graphite

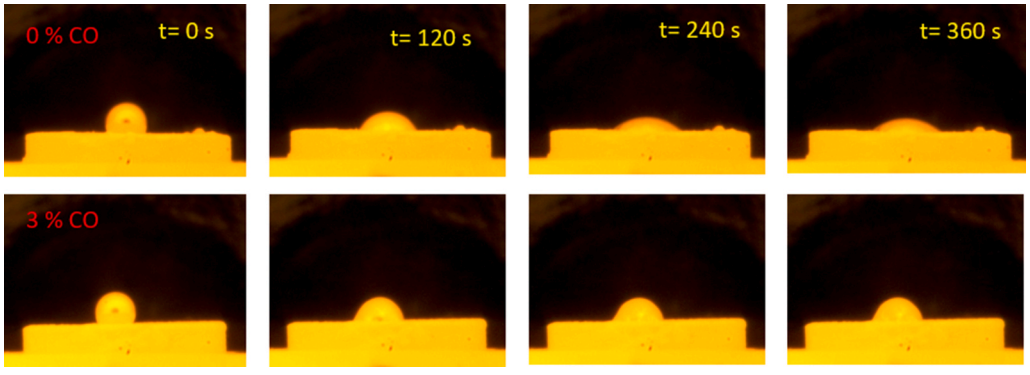

Fig. 2. Effect of CO concentration in argon on the contact angle of Si on unoxidized coated graphite substrates during isothermal holding at 1723 K. The coating thickness is 200 ± 30 μm.

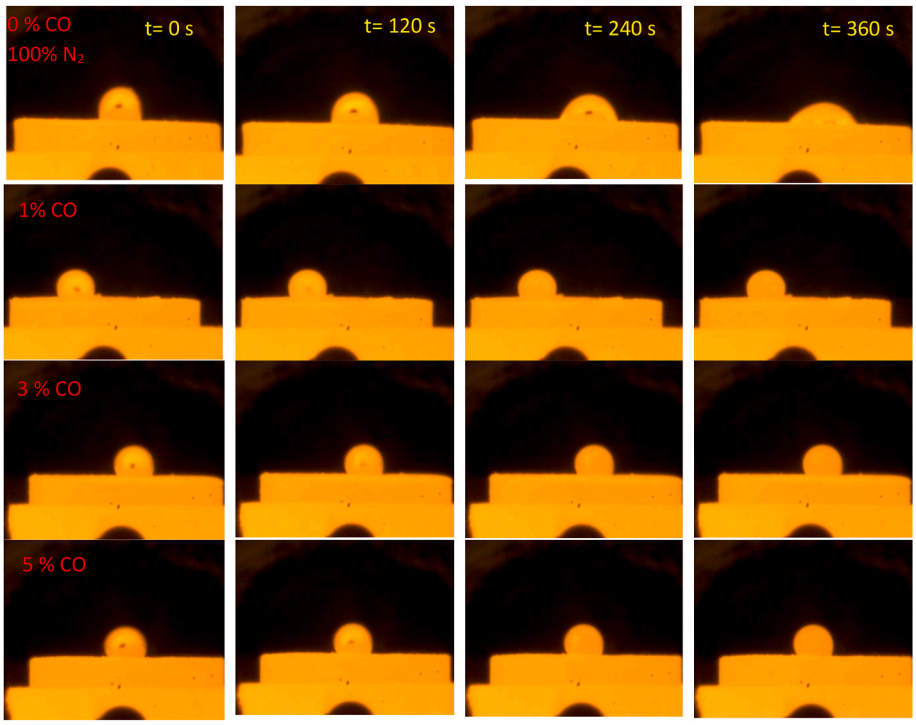

Fig. 3. In-situ images of melting silicon samples on coated graphite substrates at 1723 K in CO: N_2 atmospheres. The initial oxygen concentration of the coating is 8 wt.%.

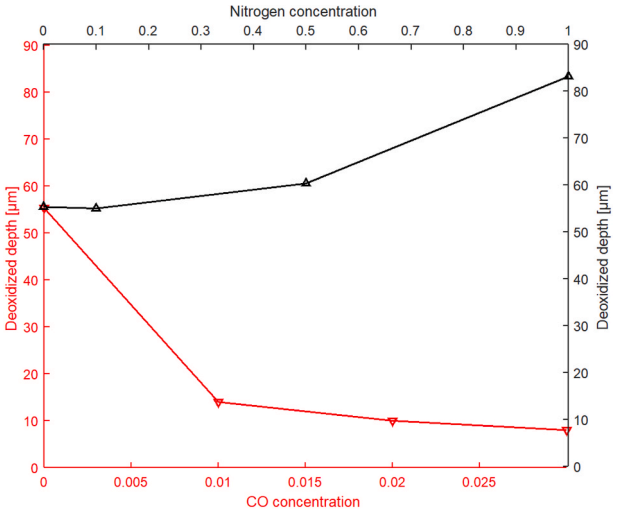

Fig. 4. Experimentally measured deoxidized depth of the coating under the droplet after 10 min of the isothermal holding at 1723 K at different CO and N_2 concentrations in the gas atmosphere (argon). The coating thickness is approximately 200 ± 30 μm. The initial oxygen concentration of the coating is 8 wt.%.

in the nitrogen atmosphere have been reported by Ref. [20] as follows:

$$2SiO_2 + 3C + N_2 \leftrightarrow Si_2N_2O + 3CO \quad (6)$$

$$3Si_2N_2O + 3C + N_2 \leftrightarrow 2Si_3N_4 + 3CO \quad (7)$$

The above reactions show that nitrogen gas does not prohibit the reduction of silica by graphite at the substrate-coating interface.

The third series of experiments (group C) was performed at different concentrations of CO in nitrogen gas to investigate the effect of both gases on the coating deoxidation process. The influence of CO on the SiO_2 decomposition under the droplet is comparable to group B samples

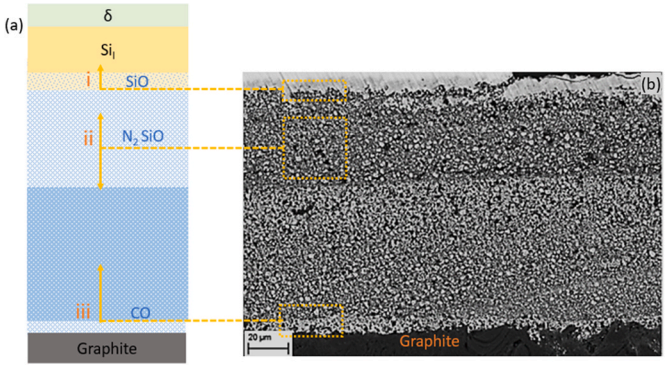

Fig. 5. The deoxidation regimes in the coating below the silicon droplet. (a) Schematic drawing that shows the gas evolution of different deoxidation (reduction) reactions. The colors from base to top correspond to graphite, deoxidized coating at the coating-substrate interface, oxidized coating, deoxidized coating in the bulk, infiltrated coating, liquid silicon, and gas diffusion boundary. (b) Electron micrograph of the coating microstructure after 30 minutes isothermal holding in argon atmosphere. (For interpretation of the references to color in this figure legend, the reader is referred to the Web version of this article.)

as shown in Fig. 7 a and b. Therefore, the existence of CO gas in the atmosphere prohibits the SiO_2 decomposition by nitrogen. Similarly, CO gas prevents the reduction of SiO_2 at the coating-graphite interface, which are represented by reactions 6 and 7.

3.3. Kinetics and mechanisms of liquid-gas reactions in the Si–N–C–O system

3.3.1. Reaction between silicon and nitrogen

Fig. 8 shows examples of the detected silicon nitride particles following the melting experiments in the nitrogen atmosphere. Silicon nitride particles are formed at the droplet surface and the liquid-coating

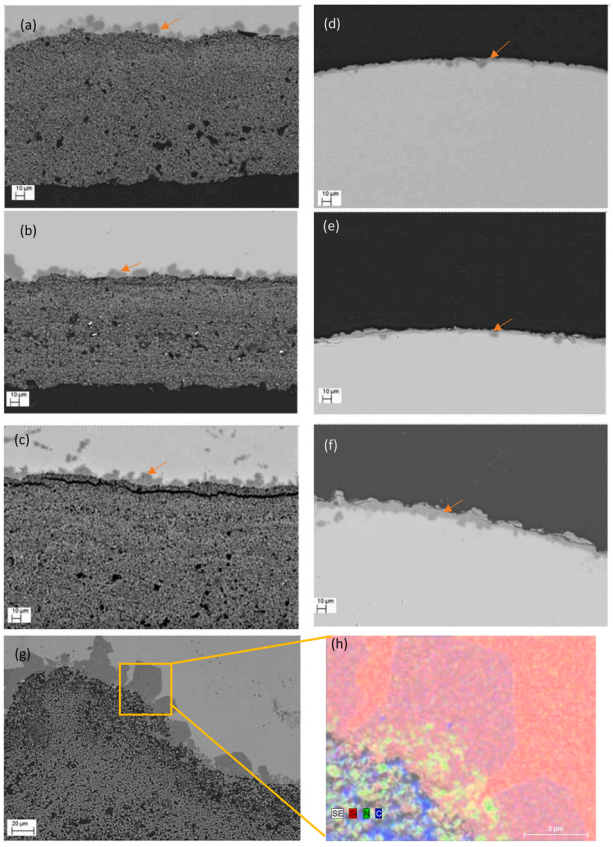

Fig. 6. (a-c) The formation of SiC particles at the liquid-coating interface after 10 min of isothermal holding at 1723 K, and at CO concentrations of 1%, 2%, and 4%, respectively. (d-f) The growth of the SiC layer at the droplet surface after 10 min of isothermal holding at 1723 K, and at CO concentrations of 1%, 2%, and 4%, respectively. (g) The morphology of the SiC layer at the liquid-coating interface at 3% CO concentration after 30 minutes holding at 1723 K with a corresponding EDS mapping of SiC particles (h). The orange arrows correspond to the SiC layer. (For interpretation of the references to color in this figure legend, the reader is referred to the Web version of this article.)

interface as shown in Fig. 8 a and b. It has been suggested by Ref. [15] that the reaction rate is linear at the early stages and the reaction constant is proportional to the nitrogen partial pressure. In the final stages, a decrease in the reaction rate is expected due to the slow diffusion of nitrogen in the nitride layer. The average diameter of the particles that formed after 30 min of the isothermal holding at 1 and 0.5 atm of nitrogen is approximately 5 μm. A careful investigation of the nitride crystals reveals that: (i) Si_3N_4 particles formation in the liquid Si is attributed to the local saturation of nitrogen, (ii) the growth of these crystals is more favorable than the nucleation of new particles, (iii) the crystals grow from the liquid surface towards the bulk silicon as illustrated in Fig. 8 a, (iv) the formation of β-Si_3N_4 is favored.

3.3.2. *Reaction between silicon and carbon monoxide*

The reaction between carbon monoxide gas and liquid silicon has been studied as a function of CO concentrations in two atmospheres: argon, and nitrogen, at 1723 K. CO gas dissolves in the liquid silicon as elemental carbon and oxygen as illustrated in Fig. 11 a. It is also expected that there will be a liquid diffusion boundary layer where the concentration of carbon is higher than in the bulk. Upon the liquid saturation of carbon, SiC particles form. A continuous carbide layer is formed at the liquid surface and the liquid-coating interface as shown in

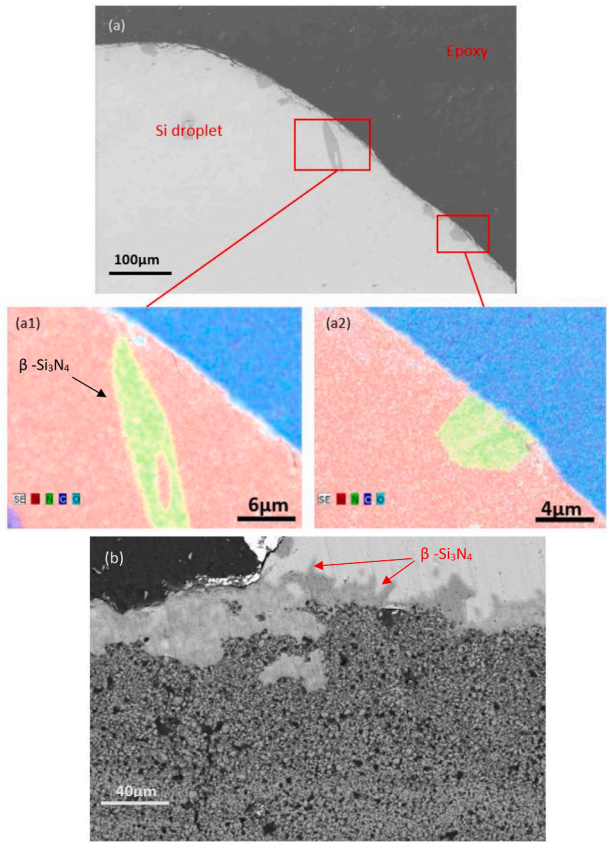

Fig. 8. (a) Examples of detected silicon nitride by EDS after 15 minutes of isothermal holding at 1723 K at a partial pressure of nitrogen 1 atm. The red is silicon, the green is nitrogen, and the blue is carbon. (b) The formation of silicon nitride in the vicinity of the triple line at a partial pressure of nitrogen 0.5 atm. (For interpretation of the references to color in this figure legend, the reader is referred to the Web version of this article.)

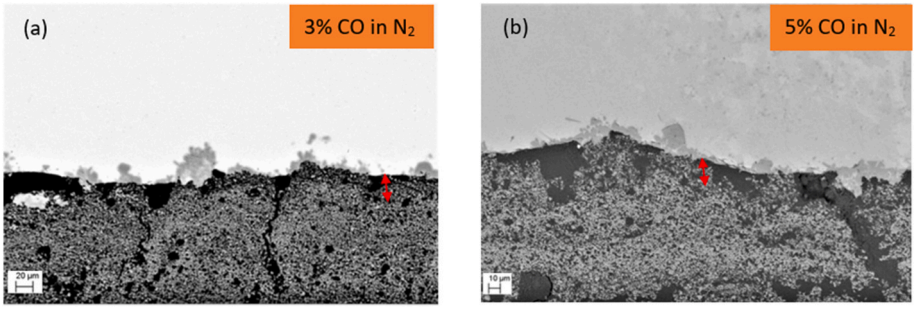

Fig. 7. The liquid-coating interface after 30 minutes of the isothermal holding at 1723 K in CO: N_2 atmosphere. The red arrows correspond to the deoxidized depth. (For interpretation of the references to color in this figure legend, the reader is referred to the Web version of this article.)

Fig. 6 (a-h). A fine-grained β-SiC layer is formed at the droplet surface as shown in Fig. 6 (d-f), and a coarser-grained β-SiC layer is found at the Si-coating interface (see Raman spectra in the Supplementary materials Figure S3). The EDS mapping of the coarse SiC particles at the liquid-coating interface reveals their high tendency to nucleate on Si_3N_4 coating particles as shown in Fig. 6 g and h. The thickness of the formed SiC at the liquid surface at different CO concentrations was measured from Fig. 6 (d-f) and plotted in Fig. 9 a. The SiC thickness is proportional to the concentration of CO in the argon atmosphere. The thickness of the silicon carbide layer, which is formed on the droplet surface, is measured at three intervals: 10, 30, and 60 minutes as revealed in Fig. 9 b. The carbide formation rate (the slope of the linear line) decreases with time. This indicates that there are two main stages of the Si–C reaction: (i) rapid reaction after the liquid saturation of carbon, (ii) slow reaction rate, which is attributed to the slow diffusion of CO through the carbide layer.

The interaction between liquid silicon and CO gas in the presence of nitrogen is more complicated than the previous case as both gases react with the liquid silicon (see the predominance diagram in Supplementary materials). According to the thermodynamic calculations at the tested partial pressures of nitrogen and carbon monoxide, the formation of SiC is more favorable than the formation of silicon nitride. However, both compounds are detected at different concentrations of CO in nitrogen. Fig. 10 shows two samples that were subjected to the same CO concentration in two different atmospheres. Fig. 10 a reveals a continuous silicon carbide layer at the droplet surface that formed due to the CO–Si interactions in argon atmosphere. Discrete SiC and Si_3N_4 particles are detected on the silicon surface that was melted in CO - N_2 atmosphere as shown in Fig. 10 b. It is clear that the formation rate of SiC decreases in the presence of nitrogen, which might be related to the increase in the carbon solubility in nitrogen saturated liquid silicon [21].

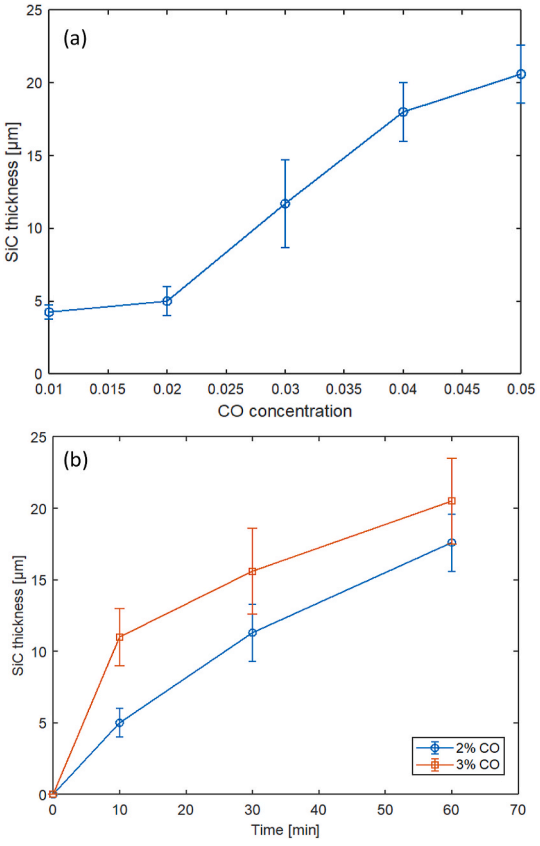

Fig. 9. The SiC layer thickness as a function of CO concentration in argon atmosphere (a), and time (b). at the liquid surface at 1723 K.

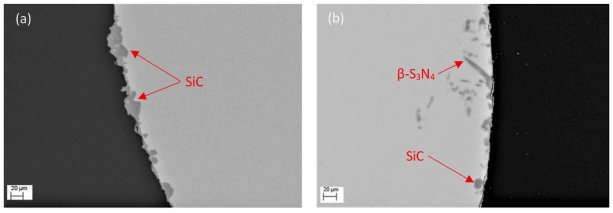

Fig. 10. Curst formation at the droplet surface: (a) SiC layer at 4% CO in argon, (b) SiC and Si_3N_4 particles at 4% CO in nitrogen. Holding time is 30 min at 1723 K.

3.4. Discussions on the effect of silicon nitride and silicon carbide on liquid infiltration and spreading

It is crucial to highlight the effect of Si_3N_4 and SiC formation on silicon wetting and infiltration. As shown in Fig. 6, the carbide layer at the liquid front prevents liquid infiltration into the coating. This observation agrees with the silicon crystallization experiments in G1 graphite crucibles that have been conducted by Camel et al. [10]. They have shown that the formation of silicon carbide at the liquid-coating interface prevents the liquid infiltration and acts as a secondary crucible that protects the graphite crucible. We showed in a previous study [19] that the change in the contact angle between the droplet and the coating is linked to the change in the chemical composition of the coating at the triple line. The decomposition of silicon oxide and silicon oxynitride promotes silicon spreading and results in a dramatic decrease in the contact angle. In the presence of CO, decomposition of these compounds is negligible at the triple line, which also represents the melt line in the large crucibles. The results of the silicon melting on unoxidized coatings in CO atmosphere show that silicon carbide formation takes place during the early stages of the melting. The rate of silicon carbide formation was higher than the wetting rate of silicon on the deoxidized samples. The formation of the carbide layer at this early stage prevents any further decrease in the contact angle and retains the droplet at a non-wetting contact angle (>90°) as illustrated in Fig. 12. This phenomenon was not observed by melting the samples in the nitrogen atmosphere. The slow formation rate of silicon nitride, compared to the carbide formation rate, does not prohibit the spreading and infiltration of the liquid silicon. In this case, the decrease in the contact angle during holding precedes the formation of a protective nitride layer. Furthermore, nitrogen gas accelerates the decomposition rate of SiO_2, as shown earlier, which in turn accelerates the wetting rate (see the schematic drawing in Fig. 12). At the liquid front, the formation of a silicon nitride layer was not as continuous and uniform as the silicon carbide layer, so infiltration of liquid silicon is not completely avoided as shown in Fig. 12 (also see Figure S4 in Supplementary materials). Camel et al. [9] have claimed that the formation of a silicon nitride layer at the liquid front, due to the dissolution of silicon nitride coating into the liquid, acts as a secondary crucible that prevents the liquid infiltration. It is noteworthy that this layer should have special features to act as a protective layer such as continuity and stability during the melting process. These features have been observed in the silicon carbide layer that formed in all the samples of group B as illustrated in Fig. 11 a-b. However, only discrete Si_3N_4 particles are observed in the samples melted in the nitrogen atmosphere (group A), as illustrated in Fig. 12 (see Figure S4 in Supplementary materials). A non-continuous layer composed of Si_3N_4 and SiC particles is observed in samples melted in CO: N_2 (group C), which does not prevent the spreading of liquid Si, as illustrated in Fig. 11 c-d (see Figure S4 in Supplementary materials).

4. Conclusions

In this study, the influence of nitrogen and carbon monoxide gases on the stability of the oxide products in the coating and the behavior of the

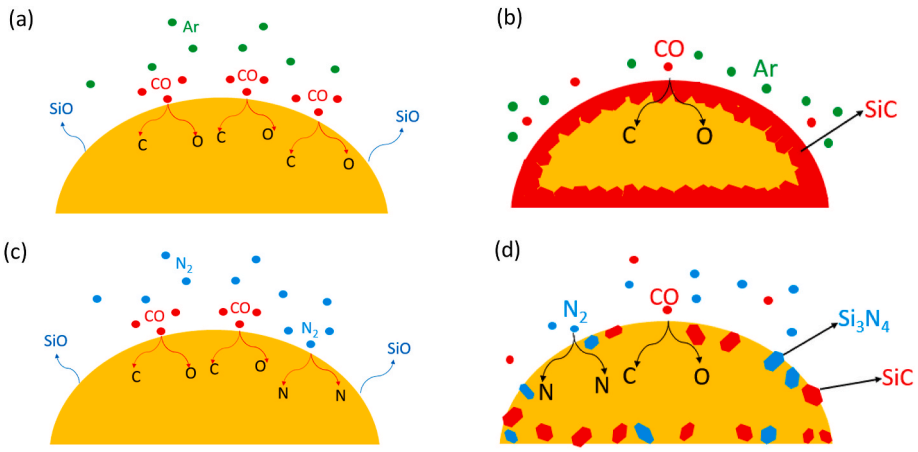

Fig. 11. Schematic drawings of CO–N_2–Si interactions during the isothermal holding at 1723 K for 30 min. (a) Early-stage CO dissolution in silicon droplet and SiO evaporation. (b) formation of the silicon carbide crust on the droplet surface, slow diffusion of CO in the carbide layer, and shrinkage in the droplet size. (c) Early-stage CO and N_2 dissolution in the silicon droplet. (d) Formation of Si_3N_4 and SiC particles at the liquid surface.

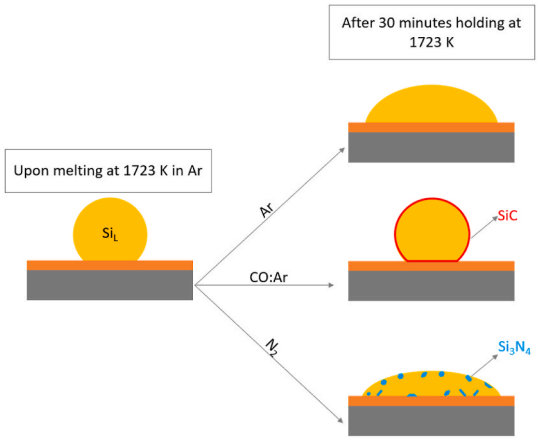

Fig. 12. Schematic drawing of the droplet shape after 30 min holding at 1723 K in different gas atmospheres. (see the attached videos for more clarification).

liquid silicon were investigated. The rapid formation of SiC at the liquid surface due to the CO dissolving in the melt maintains the shape of the droplet at high contact angle. The formation of SiC at the liquid front protects the porous coating from liquid infiltration. Furthermore, CO gas prohibits the decomposition of SiO_2 as it acts as an oxidizing agent in the atmosphere. On the other hand, nitrogen accelerates the decomposition of silica and hence, the liquid spreading and infiltration. It also promotes the formation of highly wetted silicon nitride at the triple line, which negatively affects the contact angle of silicon. The effect of CO on the coating deoxidation seems the same in argon or nitrogen atmospheres. The distribution of the precipitates in the droplets indicates that the liquid is locally saturated at the surface and the liquid-coating interface. The precipitation at the liquid front prevents the sticking of silicon on the coating and facilitates ingot removal. Based on these findings, proper control of the composition of the furnace atmosphere is beneficial to enhance the performance of the coating and prolong the lifetime of the crucibles.

Declaration of competing interest

The authors declare that they have no known competing financial interests or personal relationships that could have appeared to influence the work reported in this paper.

Acknowledgments

This work was performed within the project Crucibles for Next Generation High-Quality Silicon Solar Cells (CruGenSi), with contract number 268027 and funded by the Research Council of Norway and industry partners.

Appendix A. Supplementary data

Supplementary data related to this article can be found at https://doi.org/10.1016/j.solmat.2021.111452.

References

[1] C. Huguet, C. Dechamp, R. Voytovych, B. Drevet, D. Camel, N. Eustathopoulos, Initial stages of silicon–crucible interactions in crystallisation of solar grade silicon: kinetics of coating infiltration, Acta Mater. 76 (2014) 151–167.
[2] B. Drevet, O. Pajani, N. Eustathopoulos, Wetting, infiltration and sticking phenomena in Si 3N 4 releasing coatings in the growth of photovoltaic silicon, Sol. Energy Mater. Sol. Cell. 94 (2010) 425–431.
[3] C. Huguet, C. Dechamp, D. Camel, B. Drevet, N. Eustathopoulos, Study of interactions between silicon and coated graphite for application to photovoltaic silicon processing, J. Mater. Sci. 54 (2019) 11546–11555.
[4] I. Brynjulfsen, A. Bakken, M. Tangstad, L. Arnberg, Influence of oxidation on the wetting behavior of liquid silicon on Si3N4-coated substrates, J. Cryst. Growth 312 (2010) 2404–2410.
[5] Z. Li, L. Liu, W. Ma, K. Kakimoto, Effects of argon flow on impurities transport in a directional solidification furnace for silicon solar cells, J. Cryst. Growth 318 (2011) 304–312.
[6] S. Yuan, D. Hu, X. Yu, F. Zhang, H. Luo, L. He, D. Yang, Controllable nitrogen doping in multicrystalline silicon by casting under low cost ambient nitrogen, Silicon 10 (2018) 1717–1722.
[7] B. Drevet, A. Selzer, V. Brizé, R. Voytovych, D. Camel, N. Eustathopoulos, Chemical stability of silicon nitride coatings used in the crystallization of photovoltaic silicon ingots. Part II: stability under argon flow, J. Eur. Ceram. Soc. 37 (2017) 75–82.
[8] A. Selzer, V. Brizé, R. Voytovych, B. Drevet, D. Camel, N. Eustathopoulos, Chemical stability of silicon nitride coatings used in the crystallization of photovoltaic silicon ingots. Part I: stability in vacuum, J. Eur. Ceram. Soc. 37 (2017) 69–74.
[9] D. Camel, B. Drevet, V. Brizé, F. Disdier, E. Cierniak, N. Eustathopoulos, The crucible/silicon interface in directional solidification of photovoltaic silicon, Acta Mater. 129 (2017) 415–427.
[10] D. Camel, E. Cierniak, B. Drevet, R. Cabal, D. Ponthenier, N. Eustathopoulos, Directional solidification of photovoltaic silicon in re-useable graphite crucibles, Sol. Energy Mater. Sol. Cell. 215 (2020) 110637.
[11] Y. Yatsurugi, N. Akiyama, Y. Endo, T. Nozaki, Concentration, solubility, and equilibrium distribution coefficient of nitrogen and oxygen in semiconductor silicon, J. Electrochem. Soc. 120 (1973) 975.
[12] T. Carlberg, Calculated solubilities of oxygen in liquid and solid silicon, J. Electrochem. Soc. 133 (2019) 1940–1942.
[13] F. Durand, J.C. Duby, Carbon solubility in solid and liquid silicon—a review with reference to eutectic equilibrium, J. Phase Equil. 20 (1999) 61.
[14] H. Dalaker, Solubility of carbon and nitrogenin the silicon rich part of the Si–C–N–B-system, in: Norges Teknisk-Naturvitenskapelige Universitet, Fakultet for Naturvitenskap Og Teknologi, Institutt for materialteknologi, 2009.

[15] H.M. Jennings, B.J. Dalgleish, P.L. Pratt, Reactions between silicon and nitrogen, J. Mater. Sci. 23 (1988) 2573–2583.
[16] J.F. White, L. Ma, K. Forwald, D. Sichen, Reactions between silicon and graphite substrates at high temperature: in situ observations, Metall. Mater. Trans. B 45 (2014) 150–160.
[17] B. Drevet, R. Voytovych, R. Israel, N. Eustathopoulos, Wetting and adhesion of Si on Si3N4 and BN substrates, J. Eur. Ceram. Soc. 29 (2009) 2363–2367.
[18] F. Millot, V. Sarou-Kanian, J.C. Rifflet, B. Vinet, The surface tension of liquid silicon at high temperature, Mater. Sci. Eng., A 495 (2008) 8–13.
[19] R. Hendawi, A. Ciftja, L. Arnberg, M. Di Sabatino, Kinetics of silicon nitride coatings degradation and its influence on liquid infiltration in PV silicon crystallization processes, Sol. Energy Mater. Sol. Cell. 230 (2021) 111190.
[20] S. Baba, T. Goto, S.H. Cho, T. Sekino, Effect of nitrogen gas pressure during heat treatment on the morphology of silicon nitride fibers synthesized by carbothermal nitridation, J. Asian Ceram. Soc. 6 (2018) 401–408.
[21] H. Dalaker, M. Tangstad, The interactions of carbon and nitrogen in liquid silicon, High Temp. Mater. Process. 33 (2014) 363–368.